Université Grenoble Alpes
PhITEM

Master 1 internship report
Master Atmosphere Climate and Continental Surfaces (2018-2019)

Post-processing and analysing GNSS records of glacier motion in Svalbard in relation to a potential hydrometeorological forcing

Adrien Wehrlé

Supervisor:
Thomas Vikhamar Schuler

29th April 2019 — 28th June 2019

OSUG

Observatoire des Sciences de l'Univers de Grenoble

UNIVERSITÉ Grenoble Alpes

GRENOBLE UFR PhITEM

Master Sciences de la Terre et de l'Environnement

Attestation de non plagiat

Je soussigné(e) (Prénom NOM)

Adrien WEHRLE

Auteur du mémoire (Titre)

Post-processing and analysing GNSS records of glacier motion in Svalbard in relation to a potential hydrometeorological forcing

Déclare sur l'honneur que ce mémoire est le fruit d'un travail personnel et que je n'ai ni contrefait, ni falsifié, ni copié tout ou partie de l'œuvre d'autrui afin de la faire passer pour la mienne.

Toutes les sources d'information utilisées et les citations d'auteur ont été mentionnées conformément aux usages en vigueur.

Je suis conscient(e) que le fait de ne pas citer une source ou de ne pas la citer clairement et complètement est constitutif de plagiat, et que le plagiat est considéré comme une faute grave au sein de l'Université, pouvant être sévèrement sanctionnée par la loi.

Fait à ERSTEIN,

Le 18/07/19

Signature de l'étudiant(e)

Acknowledgments

I would like to thank Thomas, my training supervisor, who encouraged me to follow my ideas and helped me to carry them out.
I also would like to thank my colleagues Hester Jiskoot, Chloé Scholzen, Pierre-Marie Lefeuvre, Martin Hölzle, Bas Altena, Michael Angelopoulos, Luc Girod, Christopher Nuth and all the team for their precious advice and kindness.
Finally, I would like to thank Olivier Gagliardini who accepted to be the external reviewer for my internship.

Abstract

Glacier dynamics remain a major source of uncertainty in sea level rise predictions (Stocker et al., 2013) and therefore still need to be better understood in places like Svalbard, known as one of the most climatically sensitive regions in the world (Rogers et al., 2005). In this study, the potential of long-term GNSS records at Holtedahfonna ice field and Etonbreen glacier is investigated to study short-term velocity events. Three automatic methods were developed in order to post-process the data as objectively as possible by getting rid of thresholds fixing. To this end, the data behaviour has been studied with regard to a range of parameterisations and the help of the elbow method (Satopaa et al., 2011). The comparison of the resulted daily velocities showed slight but unexpected variations depending on the method used. These methods have then been compared to others used in previous studies (Helbing (2005); Sugiyama et al. (2015)) which brought into light a high sensitivity of the data depending on the post-processing. Thereafter, a temporal resolution increase revealed a first change in the data behaviour of Holtedahlfonna ice field at an eight-hour and twelve-hour resolution (for respectively 2011 and 2012) while studying the developed methods independently but also among themselves. Finally, a glaciological interpretation consisting in the comparison a mean daily velocity to surface mass balance model outputs showed that even at this scale, various processes associated with a potential hydrometeorological forcing can ben explained. It is therefore highly encouraging for further temporal resolution investigations and thus, for a better understanding of short-term glacier dynamics.

Résumé

La dynamique des glaciers demeure une source majeure d'incertitudes concernant les prévisions de la hausse du niveau des océans (Stocker et al., 2013) et par conséquent nécéssite d'être mieux comprise dans des régions comme le Svalbard, posséedant l'un des climats les plus sensible au monde (Rogers et al., 2005). Dans cette étude, le potentiel de mesures GNSS de longue durée enregistrées sur le champ de glace d'Holtedahlfonna et le glacier d'Etonbreen est évalué afin d'étudier les variations de vitesse à court terme. Trois méthodes automatiques ont été dévelopées afin de post-traiter les données de la manière la plus objective possible en s'éloignant du choix habituel des seuils. Pour cela, le comportement des données a été étudié en fonction de la paramétrisation choisie grâce à la méthode du coude (Satopaa et al., 2011). La comparaison des vitesses journalières résultantes des différentes méthodes a montré des variations faibles mais inattendues. Ces méthodes ont été comparé à d'autres utilisées dans de précédentes études (Helbing (2005); Sugiyama et al. (2015)) ce qui a dévoilé une forte sensibilité des données en fonction du post-traitement. Par la suite, une augmentation de la résolution temporelle a révélé un premier changement dans le comportement des données du champ de glace d'Holtedahlfonna à des résolutions de huit et douze heures (pour 2011 et 2012 respectivement) en comparant les méthodes de manière indépendante mais également entre elles. Enfin, une interprétation glaciologique consistant en la comparaison d'une vitesse moyenne avec des résultats d'un modèle de bilan de masse a montré que déjà à cette résolution, différents processus associés à un potentiel forçage hydrométéorologique peuvent être expliqués. Ces résultats sont très encourageants pour de futures études de la résolution temporelle et par conséquent, pour une meilleure compréhension de la dynamique des glaciers à court terme.

Contents

1 Introduction **3**

1.1 Background and theory . . . 3

1.2 Svalbard and target glaciers . . . 4

2 Data **4**

2.1 Holtedahlfonna ice field . . . 4

2.2 Etonbreen glacier . . . 5

3 Methods **6**

3.1 Developed methods . . . 7

3.1.1 Standard deviations filtering (SDF) . . . 7

3.1.2 Ratio filtering (RF) . . . 7

3.1.3 K-means filtering (KMF) . . . 7

3.2 Applied methods . . . 8

3.2.1 Exponential weighted smoothing (EWS) . . . 8

3.2.2 Gaussian weighted smoothing (GWS) . . . 8

3.3 Methods comparison . . . 8

3.4 Temporal resolution investigation . . . 9

3.4.1 Glaciers representative displacement . . . 9

3.4.2 Features analysis . . . 9

3.4.3 Temporal resolution increase . . . 9

4 Results **10**

4.1 Post-processing performance on daily velocity data . . . 10

4.1.1 Developed methods similarity . . . 10

4.1.2 Comparison with applied methods . . . 11

4.2 Performance at higher temporal resolutions . . . 12

5 Discussion **15**

5.1 Contribution of melt-enhanced sliding to overall glacier displacement . . . 15

5.2 Glaciological interpretation . . . 15

5.3 Improvements and perspectives . . . 18

6 Conclusion **18**

7 Appendices **22**

1 Introduction

1.1 Background and theory

Glaciers are among major contributors to global sea-level rise in the 20th and 21th century (Vaughan et al., 2013). More specifically, glaciers and ice caps contribute more than the Antarctic and Greenland Ice Sheet despite their small volumes (Church et al., 2011). This contribution is divided in two components: changes in surface mass balance and changes in dynamics (e.g. accelerated flow, lake or tidewater calving). Changes in the dynamics of glacier flows have important implications for glacier mass balance (Dunse et al., 2012). Indeed, such accelerations result in an increase of ice melt and iceberg calving in the case of tidewater glaciers. Its potential contribution to sea level rise is suggested to account up to 2 meters by 2100 (Pfeffer et al., 2008).

Glacier dynamics, especially during the summer melt season, have been widely documented allowing to understand the relations between surfaces processes and bed sliding (e.g. Zwally et al. (2002);Shepherd et al. (2009)). Thus, the surface melt produced at this season added to rainfalls evolves in different ways on and in glaciers: part of it flows along supgraglacial rivers and can be stored in supgraglacial lakes. These lakes can suddenly drain and trigger an acceleration of the glacier motion when the water reaches the bed (Das et al., 2008). Another part percolates through the surface firn layer (Cuffey and Paterson, 2010). Finally, the biggest part is brought by moulins and crevasses towards subglacial hydrological systems where it can enhance the glacier motion (Cuffey and Paterson, 2010).

Even if these processes are well documented, glacier dynamics are still a major source of uncertainty in sea level rise predictions (Stocker et al., 2013) and thus, still need to be better understood.

As a consequence, along with modelling and remote sensing, field investigation is known as one of the key to study these processes. GNSS (Global Navigation Satellite System) positioning progressively became one of the most important tool to survey the Earth surface variations since its appearance in the 1980s (Hofmann-Wellenhof et al., 2007). Glaciologists were amongst the first to adopt this technology (e.g. Hinze and Seeber (1988)) due to the disadvantages of traditional methods (King, 2004). Indeed, despite the high precision of older survey methods using theodolites and geodimeters (e.g. Hooke et al. (1989)), GNSS measurements have been acknowledged as much more efficient when it comes to large area covering and continuous monitoring. Coupled with glacier motion survey, this technique helped to understand some important processes as e.g. hydraulic jacking resulting in glacier uplift (Bartholomew et al., 2010) or spatial strains variations along a glacier surface (Harper et al., 2007). Besides, many studies has been lead in relation to short-term velocity variations (e.g. Flowers et al. (2016); Sugiyama et al. (2015)) but only a few were based on long-term records.

Here, it is proposed to work with long-term records of glacier motion in Svalbard in order to explore the measurements potential when it comes to analysing short-term acceleration events. Indeed, these events are still misunderstood as a result of their obviously short durations making them challenging to record.

The focus has been mainly set on the data mining part with the aim of developing post-processing methods and comparing them to existing ones in order to improve the results objectivity. Indeed, the main problematic investigated here is the link between the level of post-processing and the confidence that can be put in the resulting data. Without any controlling or reference data (e.g. measurements with other instruments), post-processing in the most objective way becomes challenging, even more when high temporal resolutions are targeted. Then, the resulting velocity time series that have not been investigated in details until now, are analysed from a glaciological perspective. A quantification of the contribution of the melt season displacement to the overall displacement is presented and possible relations to hydrometeorology are hypothesized.

1.2 Svalbard and target glaciers

The Svalbard archipelago is situated in the High Arctic, North of Norway, between 75 and 81°N. The total islands area is 60 000 km^2, 57% covered by glaciers (Nuth et al., 2013). The meteorological conditions of this region are known as spatially and temporally diverse (Hisdal, 1998) due to its location where warm and moist air coming from the South meets drier air masses originated from North-East (Käsmacher and Schneider, 2011). Besides, Svalbard is known as one of the most climatically sensitive regions in the world (Rogers et al., 2005). The eastern side of the Archipelago is characterized by smoothed reliefs and low-altitude ice caps while the western part exhibits an alpine topography (Østby et al., 2017). Most glaciers and ice caps are considered to be polythermal (e.g. Björnsson et al. (1996)) and more than 60% of the glaciated areas are glaciers which terminate in the sea at calving icecliffs, known as tidewater glaciers (Błaszczyk et al., 2009). Despite typical slow velocities $< 10m.y^{-1}$ (Hagen et al., 2003), frequent surges have been observed as documented e.g. in Lefauconnier and Hagen (1991), and more recently in Dunse et al. (2015). Holtedahlfonna, the first study site, is the largest ice field on the island of Spitsbergen covering $\sim$ 300km^2 (Ruppel et al., 2014) and situated 40km northeast of Ny-Ålesund research station (see Figure 1). It is classified as a polythermal glacier (Christianson et al., 2015) covering an altitude range of 0-1441 m a.s.l. (NPI, 2014) with a thickness up to $\sim$ 650m (Bahr, 2015). It drains into Kronebreen, one of the fastest marine-terminating glaciers in Svalbard with annual frontal ablation between 0.2 and 0.5 $km^3.a^{-1}$ within the past 15 years (Schellenberger et al., 2014) corresponding to 96% of the annual ice loss of the glacier (Nuth et al., 2012). It is important to point out that the boundary between the two systems is still slightly uncertain in space and time (Nuth et al., 2012). While Kronebreen is a well-studied glacier, fewer studies focused on Holtedahlfonna (Lefauconnier et al. (2001); Bahr (2015)).

The second study site, Etonbreen glacier, is part of Austfonna which is a $\sim$ 8000km^2 (Moholdt et al., 2010) polythermal ice cap located on Nordaustlandet island, in the North-East of the archipelago. Most of the ice cap is slow-moving with velocities representative of the Archipelago average, less than $10m.y^{-1}$ (Dowdeswell et al., 2008) except few fast-flowing systems (see Figure 2). Several surges have been observed across the ice cap (Lefauconnier and Hagen, 1991) with the most recent one at Basin 3, in 2012 (Dunse et al., 2015). Etonbreen glacier surged in 1938 but is now slowly flowing at a rate of $\sim 3m.y^{-1}$, which is one of the reason why it is currently less studied than other glaciers of the region.

2 Data

2.1 Holtedahlfonna ice field

A long term GNSS survey has been carried out on Holtedahlfonna ice field by the Department of Geosciences of the University of Oslo (UiO) from 2011, still ongoing (see Figure 1). It is composed of 3 GNSS rover stations and 3 base stations which characteristics are presented in Table 1 (Appendices). The rover stations (named HDF1, HDF2 and HDF3) have been placed on the glacier on existing mass balance stakes of the Norwegian Polar Institute (NPI). Two of the 3 base stations (named NYA1 and NYAL) are situated at Ny-Ålesund research station and are the property of the Norwegian Mapping Authorities. Both of them are $\sim$ 29km far west from HDF1. The third base station (HAGN) has been installed during the field season of spring 2015 on a Nunatak at Kongsvegen glacier, $\sim$ 12km south of HDF1 (Bahr, 2015). It is already important to notice that the satellite coverage is reduced due to a masking effect of the surrounding reliefs, involving harder recording than usual. These installations have been particularly developed to cope as efficiently as possible with the extreme arctic climate and their remote location. In this way, each GNSS rover station is powered by a solar panel (maximum 24V, reduced to 12V to charge batteries) and 2-6 batteries ($\sim$ 180-240 Ah) chosen after an analysis of the station consumption during the winter season (Bahr, 2015). Indeed, the polar night, from October to February, is constraining the powering system much more than at

lower latitude investigation sites. While the sampling frequency is 5 seconds all day long during the summer period (from the 30^{th} of April to the 1^{st} of September), a timer integrated to the system reduces the measurement period to two hours in winter. Although installations are constantly improved, data gaps still remains due to technical problems and harsh meteorological conditions. The data available for this study (named HDF data afterwards) comes from two parts of GNSS records from 2011-05-02 to 2011-10-04 and from 2012-05-02 to 2012-09-30 at HDF1 station, projected in UTM zone 33. These two datasets have been already processed by determining hourly static solutions from raw RINEX files using the GNSS software RTKLIB (C. Nuth, unpublished data). The initial 5 seconds timestep has been kept. A summary of the variables used and described in this study is available in Table 2 (Appendices).

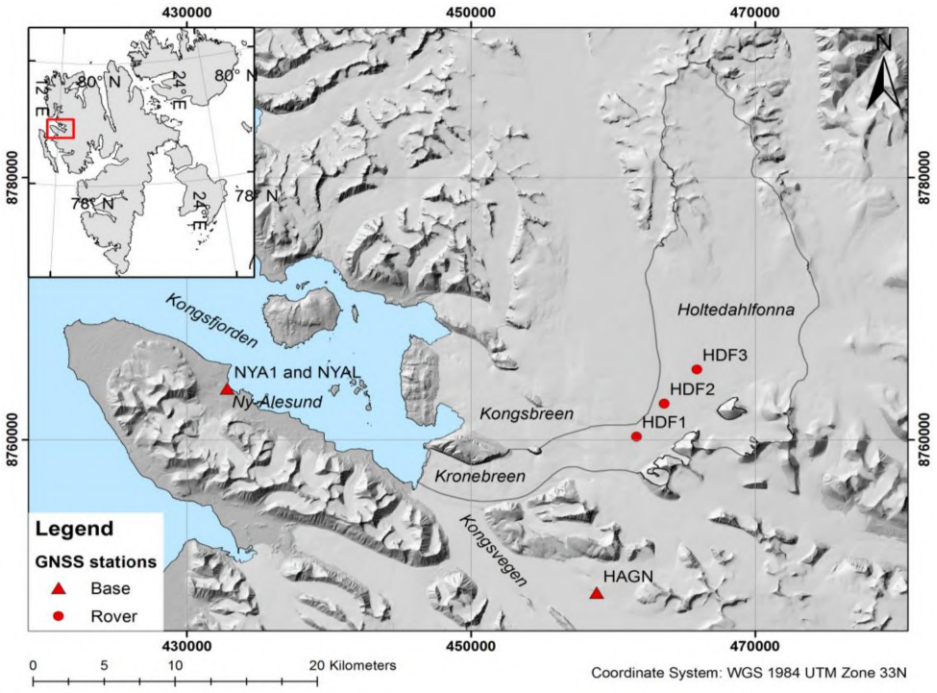

Figure 1: Overview of Holtedahlfonna ice field study area (Bahr, 2015)

2.2 Etonbreen glacier

A similar GNSS survey has been lead on Etonbreen glacier from 2014, still ongoing. This time, only one station (see Figure 2) has been installed at the location of an existing Automatic Weather Station (AWS) itself established by a team of the UiO Department of Geosciences in 2004 (Schuler et al., 2014). The station is situated in a much more open area than on Holtedahlfonna ice field, allowing a higher precision by a better satellite coverage. The powering setup is similar than the one used on Holtedahlfonna icefield, the antenna and receiver characteristics being alike HDF1 station. Two parts of records from 2014-05-06 to 2014-09-15 and from 2015-05-06 to 2015-09-15 at a 5-seconds timestep are also available, projected in UTM zone 33 (named ETB data afterwards). As for Holtedahlfonna ice field, the data has already been processed with RTKLIB but this time in kinematic Precise Point Positioning (PPP) i.e. using a single receiver signal without a base station. Only the three positioning components X, Y and Z were available. For that reason, the work and the methods development presented in Section 3.1 have been mainly carried out on HDF data and then adapted to post-process ETB data.

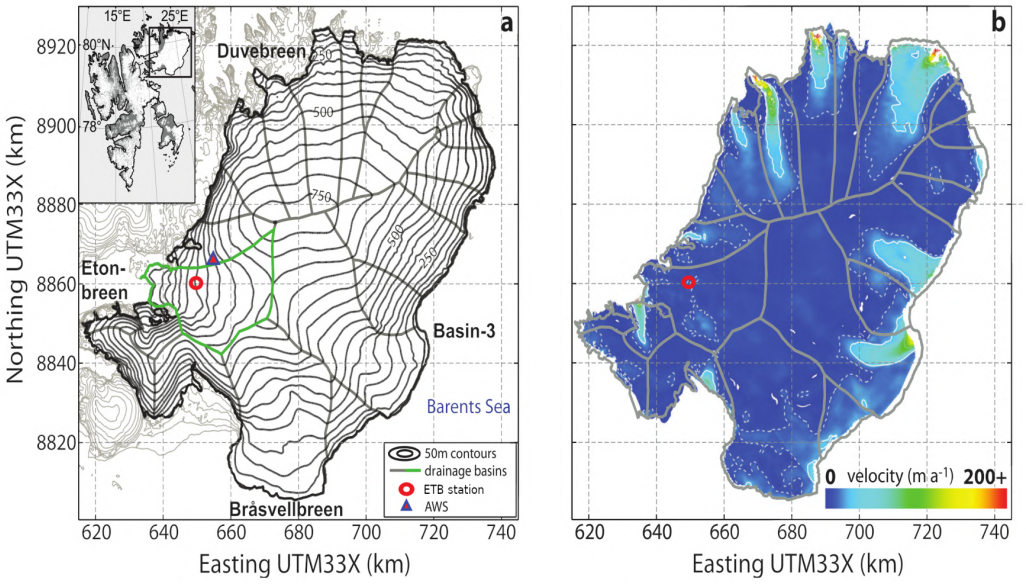

Figure 2: Overview of Etonbreen glacier study area. **a)** Surface topography of Austfonna with 50m elevation contours according to a DEM by Moholdt and Kääb (2012) showing ETB station (red circle) and a second Automatic Weather Station (AWS). The area outlined in green corresponds to the basin of Etonbreen. **b)** Surface velocity structure of Austfonna modified from Dowdeswell et al. (2008), derived from ERS-1/2 SAR scenes acquired between December 1995 and January 1996. Dashed contours indicate a velocity of $10m.y^{-1}$, solid contours are at $25m.y^{-1}$ intervals. Modified after Dunse et al. (2012).

3 Methods

In order to have a broad view of different possible post-processing results, several methods have been applied and compared to each other. All the developed methods described in Section 3.1 are filtering methods which means that at each step, part of the raw data is deleted while the rest is used for the next steps. On the other hand, the two applied methods described in Section 3.2 are smoothing methods where all the data remains but is re-evaluated with regard to the surrounding values. Initially, the two first developed methods were applied by choosing different thresholds and as a consequence, made the post-processing very subjective. In a goal of generalisation, the related thresholds fixing has been subverted as often as possible by using the elbow method. Instead of choosing one value, the methods are run for a range of values to identify possible changes in the data behaviour along the evolution of the parameter. When all combinations are plotted as a function of a representative variable, this change may result in an elbow of the curve giving an indication of a highest possible threshold before a change in the data behaviour. With the percentage of missing values as representative variable, the elbow point can be presented as a combination or a trade-off between a restrictive threshold and a percentage of missing values as low as possible. The algorithm here used is Kevin Arvai's attempt to implement the Kneedle algorithm developed by Satopaa et al. (2011) and based on the maximum curvature. Once the methods developed and the velocities compared at a given resolution of twenty four hours, the goal was to investigate the different post-processing performances when it comes to increase the temporal resolution.

3.1 Developed methods

3.1.1 Standard deviations filtering (SDF)

The first developed method have been motivated by a preliminary work done on the data (C. Nuth, unpublished). The first step consists in an ambiguities resolution check using the variable Q. All the values that have a Q value of 1 are kept, meaning that the phase ambiguities have been solved by the processing in RTKLIB.
Then, the data is filtered based on the standard deviations computed by RTKLIB, representing the estimated standard deviations of the solution assuming a priori error model and error parameters by the positioning options (Takasu, 2013). A global variable has been set by determining the square root of the summed squared standard deviations of each component (X, Y and Z), at each timestep. The optimal threshold on this variable is determined by applying the elbow method as described above with the percentage of missing days on a window from 0 to $mean + 3\sigma$.
Finally, the last step focuses on the station positioning through time. A linear regression of the station track is first computed in order to determine the related residuals (r). In the case of a station that does not have a linear displacement, a rolling linear trend can be used. Then, knowing that the shortest distance to the linear trend of a given slope (s) is the perpendicular to the latter, the minimum distance (d_{min}) of each point to the linear trend is determined by trigonometric relations as follows: $d_{min} = sinus(1 - s) * r$. A z-transformation is then applied to these distances consisting in subtracting all distances by the mean and dividing by the standard deviation. A threshold had to be chosen in order to keep only the values closer to a certain distance to the linear trend and has been fixed at 1 σ.
The velocity is lastly calculated by taking mean positions of 2 consecutive windows. It was therefore necessary to calculate a mean time for all mean positions (daily positions for the first case). Indeed, for two consecutive windows, the velocity was initially computed by dividing the displacement by the window size. Unfortunately, if the values remaining from the post-processing have been recorded at the end and the beginning of the first and second window respectively, the velocity would have been under-estimated as it is based on a wrong duration. To this end, a function detects the time of all remaining values and determine a mean time to compute a more realistic duration.

3.1.2 Ratio filtering (RF)

The second filtering method is based on the ratio variable which is the ratio of squared residuals between the best integer vector to the second-best vector (first and second best solutions) computed by RTKLIB (Takasu, 2013). During a preliminary manual data mining work, it has been shown that the ratio variable seems to be a relatively strong variable for the data post-processing helping to delete outliers but also possible bad quality data at shorter time scales.
In this way, the first step of this method consists in a filter on this variable. As for the SDF method, the threshold is fixed by applying the elbow method on the percentage of missing values. The second step is the same processing in regards to the linear trend as for the SDF method, the velocity has also been computed similarly.

3.1.3 K-means filtering (KMF)

The last method has been developed in a desire to evaluate each measurement as a whole by taking into account different variables at the same time instead of filtering step by step. To this end, the K-means unsupervised classification (MacQueen et al., 1967) has been used. K-means clustering is a basic machine learning method commonly used to automatically partition a data set into k groups (Wagstaff et al., 2001) based on n variables. It proceeds by choosing k initial cluster centers called centroids, in the n-dimensional space created by the data. By computing the Euclidean distance between all points and centroids, the closest centroid is attributed to each point.

Then, cluster centers are recomputed to be the barycentre of their respective data groups. Finally, the algorithm iterates and converges when the cluster centers are non longer updated. While the relations between the variables can be manually determined in two or three-dimensional spaces, one of the advantage of the K-means algorithm is that it can investigate them at higher and non-representable dimensions.
Here, six variables are used i.e. the standard deviations on each component (X, Y and Z), the ratio and the number of satellites. The last variable is the z-score determined in the same way as in SDF and RF methods. Then, an alternative version of the elbow method has been used to determine the unknown number of clusters to partition the data (Bholowalia and Kumar, 2014). It consists in running the algorithm for different number of clusters (usually from 1 to 10) and computing the related Sum of Squared Error (SSE). By plotting this variable as a function of the clusters number, the optimal number of clusters is the elbow of the curve. As a result of the data characteristics, all the values that are deleted are stored in one cluster while the others contain the remaining data.
It has been quickly discovered that only one cycle of clustering on the raw data resulted in a low restrictive filtering due to the presence of a significant amount of outliers. Thus, the filtered data has been filtered again 5 times and the elbow method has been used once more to select the optimal number of clustering cycles with the help of the percentage of missing values. Finally, the velocity has been determined as for the SDF method.

3.2 Applied methods

3.2.1 Exponential weighted smoothing (EWS)

The method developed by Helbing (2005) has been used to investigate the glacier dynamics of Unteraargletscher, Switzerland, by verifying theoretical concepts through flow modeling, then compared to field measurements. It is a smoothing technique that contrasts with the previous methods which were all filtering methods.
First, the linear trend over the entire observation duration has been removed for each component of the position (X, Y and Z) separately to obtain the residuals. Then, each component residuals were filtered with an exponentially decaying weighting function applied to a rolling mean.
The weight is determined as follows: $weight = exp(-1 * |dt| * width^{-1}$ with the width fixed at 1.5 days and dt the time in relation to the window center. Then, each trend have been added again to compute the horizontal velocity with the initial timestep. Finally, the velocity itself is smoothed with the help of the same function than before, with a width of 0.5 days.

3.2.2 Gaussian weighted smoothing (GWS)

The last method has been developed by Sugiyama et al. (2015) to study the glacier dynamics near the calving front of Bowdoin Glacier, northwestern Greenland by comparing satellite and field observations.
To apply it with an equivalent timestep as the initial study, the raw data used here has been resampled to 15 minutes by mean over the window. Then, a rolling mean has been applied on each raw component of the positioning with a Gaussian window type and a window size of one hour.

3.3 Methods comparison

Daily velocities obtained with each of the three developed methods on HDF data have been compared to each other. After a quantification of the deviations, correlation coefficients have been determined. The signals normality, statistically tested by the Shapiro-Wilk test, have been rejected with p-values higher than 10^{-7}. As a consequence, the non-parametric Spearman correlation has been used.
Then, the methods have been compared to a low-processed daily velocity computed with raw daily mean positions. It is used as an indicator of the level of processing but is in no way an absolute reference. To this end, the low-processed velocity has been subtracted to each velocity to obtain the related variations time series. They have been

normalized by the first to have a percentage of variations in regards to it.
Concerning ETB data, only one developed method was possibly usable due to a lack of controlling variables. As a consequence, a method similar to the SDF method has been applied but without the precision filter on the standard deviations. Thus, it only resulted in the filtering with respect to the linear trend and in the velocity determination. The elbow method has been applied to find the optimal z-score threshold as it remained the only one to determine. Finally, the mean signal from the developed methods has been compared to the applied methods.

3.4 Temporal resolution investigation

3.4.1 Glaciers representative displacement

The representative displacement of both glaciers have been studied as it has a direct influence on the possible temporal resolution of the velocity. Indeed, considering a constant measurement precision, the required time window to be able to record a real displacement will be much longer for a slow-flowing glacier like Etonbreen glacier than a faster-flowing one like Holtedahlfonna ice field. To this end, displacements and related velocities have been computed from the raw data over a time window from one hour to two days. A mean displacement and velocity over each window have been determined to study the displacement evolution as a function of the window size. Then, it has been compared to a minimum recordable displacement in order to set the higher reachable temporal resolution even before post-processing. Due to a lack of informations related to the GNSS measurements precision, this limit has been fixed at 1 centimeter which is a mean precision representative of these kind of surveys.

3.4.2 Features analysis

A work has been led on Holtedahlfonna station track to study special features consisting on clouds of positions quickly shifted from the linear trend that presumably come from the data processing (see Figure 3). It was thus essential to investigate their duration as they could highly constrain the temporal resolution. A preliminary manual study showed that fixing a threshold of 2 on the ratio variable allowed to separate these features from the raw data. Thus, a K-Means algorithm as described in Section 3.1.3 has been developed to automatically examine features one by one. The variables used to cluster the data are the horizontal positioning components X and Y. The same global variable than for the SDF method based on standard deviations has been added, suspecting a strong relation between the precision and the presence of these features. The algorithm is run each day of the dataset. Each time, the three variables are standardized by the z-transformation which consists in subtracting all values by the related mean and dividing by the standard deviation. Then, the elbow method have been applied as described for the KMF method to determine the optimal number of clusters for each day. Finally, the duration distribution of the related features have been analysed.

3.4.3 Temporal resolution increase

Each developed method has then been applied to HDF data with temporal resolutions of twelve, eight, six, three and one hour.
First, the results of the temporal resolution increase of each method have been independently studied. For each resolution, the percentage of missing values and the SNR (Signal-to-Noise Ratio) have been determined, respectively giving indications on the level of data removal and the signal signature. It is important to note that these variables are most probably not correlated with the post-processing performance and are used here only as indicators. Indeed, for example, a high percentage of missing values in the resulting velocity shows a high level of post-processing but not necessarily a high accuracy. These two variables have also been computed for the resolution increase of the low-processed velocity described in Section 3.3.
The tracking of these two variables along the resolution increase and for each method is investigated to detect

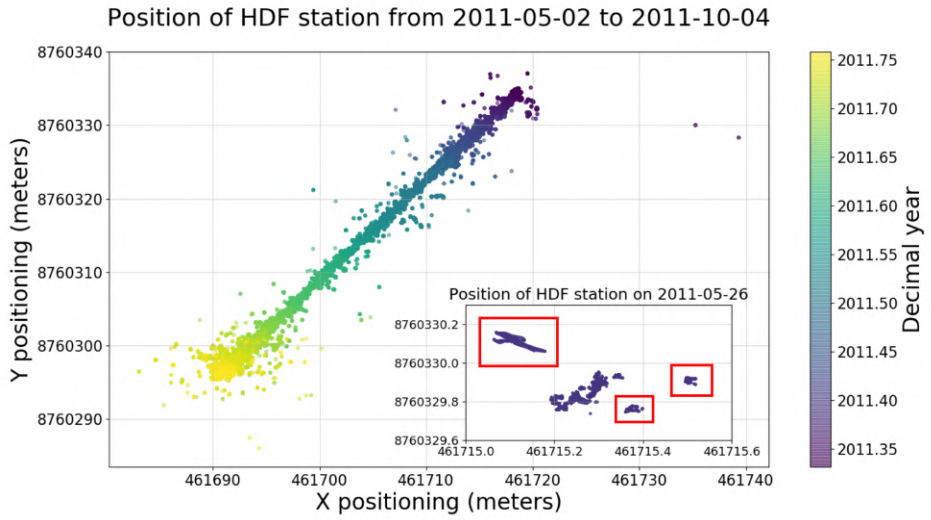

Figure 3: Holtedahlfonna ice field station track along 2011. The window focuses on the 26^{th} of May 2011 and shows examples of features targeted in section 3.4.2 (red rectangles).

possible changes in the data behaviour. With the same goal, Spearman correlation coefficients have been determined between the methods for each resolution to compare the methods among themselves.

4 Results

4.1 Post-processing performance on daily velocity data

4.1.1 Developed methods similarity

Initially, only very slight variations were expected between the different daily velocities. Indeed, at this scale and at least during the summer period, a majority of good quality measurements should remain which should give only a small influence to outliers and bad quality measurements. However, a comparison between the results of each developed method applied to HDF data showed some significant variations. Even if the mean absolute variations in regards to the average velocity of the three methods is 3% and 7.8% (for respectively 2011 and 2012), variations up to 22 % (on the 7^{th} of August 2011) of the mean velocity have been determined during the 2011 summer period (see orange span in Figure 4a) and up to 38% for the 2012 summer period. As expected, high variations up to 25 % (2011) are visible at the end of the summer due to the winter acquisition mode described in Section 2.1. In 2012, only the KMF method kept values during the pre-winter period.

Despite these short-term variations between the methods, high correlation coefficients of 0.96, 0.92 and 0.94 (2011), 0.80, 0.79 and 0.92 (2012) have been determined for respectively KMF/RF, KMF/SDF and RF/SDF which reflects an important overall similarity.

Besides, variations are visible between the developed methods and the low-processed velocity (see Figure 4b). Even if the mean percentage of the variations described in Section 3.3 is 0.6% (2011) and 2% (2012), the standard deviations are 16 % (2011) and 24 % (2012), with values up to 52 % (2011) and 34 % (2012) within the summer period. It shows a high heterogeneity of the data quality through time. Again, high variations at the end of the summer are noticeable with values up to 80 % (2011) and even 158 % (2012). These divergences can be directly linked with the smoothing effect of the three methods on the velocity, reducing the wiggling observed in the low-processed velocity (see Figure 4a). Finally, the general higher variations of 2012 HDF data than 2011 HDF data show a lower data quality in 2012. Indeed, the highest deviations come from the KMF method which is possibly

due to a glut of bad quality data, resulting in a harder clustering. This hypothesis is also strenghtened by a twofold lower average ratio value for 2012 compared to 2011.
Concerning ETB data, slighter variations than for HDF data between the velocity from the developed method and the low-processed velocity have been determined with standard deviations of 11.6 % and 8.3 % (for respectively 2014 and 2015). It is mainly due to the limited level of processing of the developed method and the absence of features as described in Section 3.4.2, making its methodology similar to the low-processed velocity one. Finally, due to their filtering characteristics it is important to notice that 7.1, 5.1 and 4.5 % (2011), 10.5, 20.3 and 14.5 % (2012) of the HDF overall data for respectively the SDF, RF and KMF method have been deleted, most of it during the pre-winter period where the data quality decreases significantly. The post-processing of ETB data resulted in percentages of 14.2 % (2014) and 10.6 % (2015).

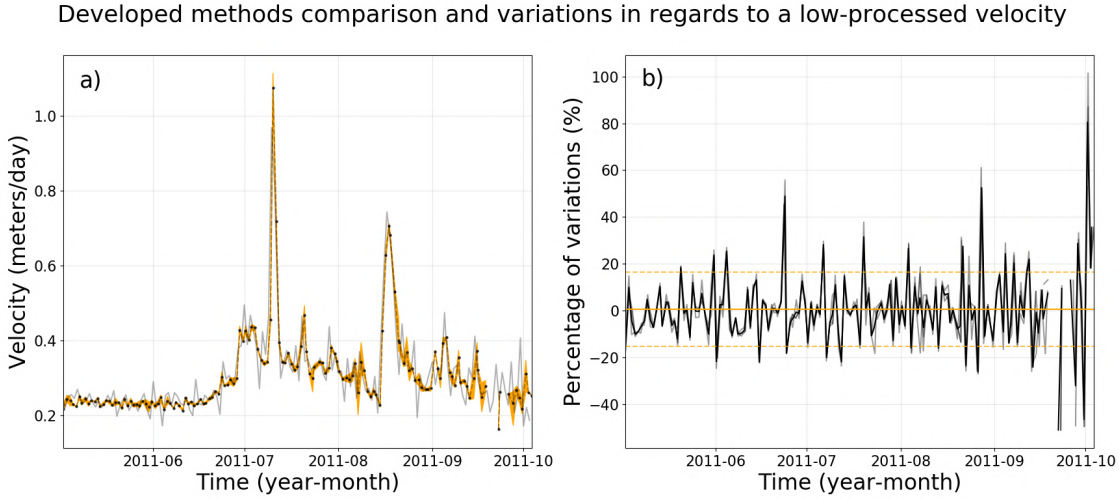

Figure 4: **a)** 2011 average velocity from the three developed methods (black dashed lines and black dots) and relative maximums/minimums (orange area). The low-processed velocity is superimposed (grey line). **b)** Percentage of variations in comparison to the low-processed velocity for each method (grey lines) and resulting average (black line). The mean percentage $+1\sigma/-1\sigma$ are respectively represented in orange line and orange dashed lines.

4.1.2 Comparison with applied methods

The EWS method results show velocities in average up to 2.5 (2011) and 2.25 (2012) times the mean velocity from developed methods for HDF data during the summer period, up to 3.2 and 2.23 times during the pre-winter period (see Figure 5a). Indeed, even if smoothed, the velocity is still computed every 5 seconds timestep which makes it unfortunately very sensitive to outliers and bad quality data. On the other hand, variations that cannot be seen in the daily velocity are here revealed. However, it is very complicated to assess the level of confidence on the results as any controlling variables are used and therefore, all measurements are processed at the same level. Indeed, without the comparison with filtering methods, it would be impossible to notice that the acceleration events during the pre-winter period, even higher than in summer, are most likely due to the bad data quality at this time.
Finally, a half day offset between the acceleration peaks of the two signals can be noticeable for both years, most likely coming from the rolling means (consecutively 1.5 and 0.5 days) that shifted the values in time.
The velocity resulting from the GWS method are even higher, up to 15.2 (2011) and 16.7 (2012) times in average during the summer period, up to 18.3 and 8.1 times during the pre-winter one (see Figure 5b). It clearly shows that the data remains under-processed which is consistent with the low level of processing. Indeed, the data is even more affected by the outliers and background noise than in the EWS method. The pre-winter period also shows accelerations led by outliers as for the EWS method. Even if these two methods have been developed for

relatively similar analysis than the one lead here, the variations in regards to the developed methods shows that the post-processing can be highly dependent on the data quality and characteristics. Indeed, for the GWS method, the raw data used in the initial study was clearer than those used for this study resulting in a light post-processing, inappropriate for the data here studied. Concerning ETB data, the EWS velocity is up to 6.2 (2014) and 9.3 (2015) times the mean velocity from developed methods, up 30.6 to 59.5 times for the GWS method. This saturation is mainly due to the velocity over-sampling coupled to the slow motion of the glacier discussed below in Section 4.2.

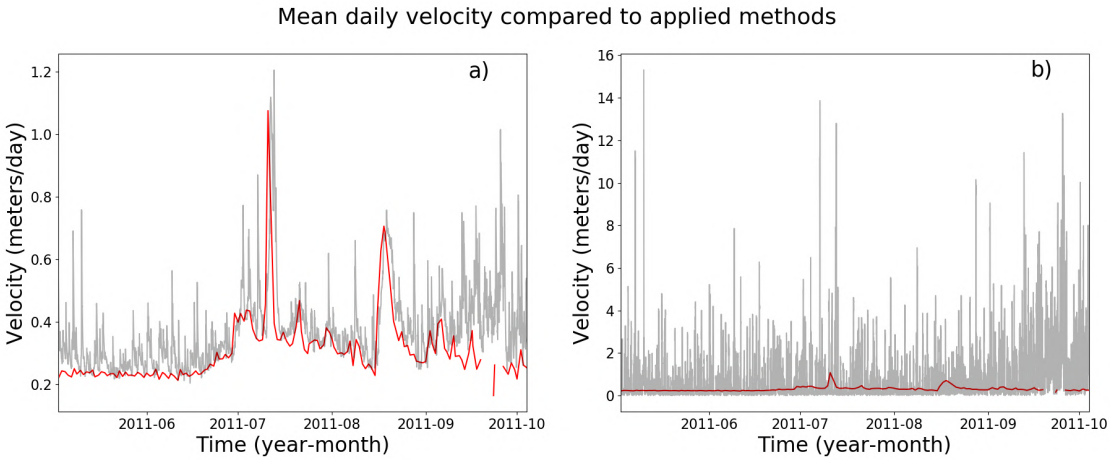

Figure 5: 2011 average velocity from the three developed methods (red lines) compared to **a)** EWS method and **b)** GWS method (grey lines).

4.2 Performance at higher temporal resolutions

The preliminary work on the glaciers representative displacements provided the evidences of the previously stated high differences between Holtedahlfonna ice field and Etonbreen glacier. Indeed, for HDF data (both years), even at the shorter duration of 1 hour (shorter window size), the mean displacement is already in average 12 times higher than the threshold (see Figure 6a). On the other hand, a duration of approximately 22 hours is needed to outreach the threshold for ETB data (see Figure 6b).

These results are directly linked to the related velocities. Indeed, the latest stabilised to an average value of $0.3m.d^{-1}$ at high window sizes for HDF data, where a much lower value of $0.01m.d^{-1}$ is reached for ETB data. Thus, it has been showed that the representative displacement of Holtedahlfonna ice field during the studied years will not compel the temporal resolution. It is the contrary for Etonbreen glacier where a temporal resolution higher than 22 hours is, in any case, not reachable because of its slow representative displacement. As a consequence, the temporal resolution increase has not been led for this data set. It is also important to notice a high velocity dependence on the window size at shorter intervals than approximately 10 hours for HDF data, 18 hours for ETB data (see Figure 6). It clearly shows a high sensitivity of the velocity to strong short-term variations which can be connected with the velocity amplitude of the applied methods.

The K-means algorithm results showed a strong occurrence of features duration around 1 hour (for 2011 and 2012) which coincides with the short-term velocity behaviour described above. Indeed, among a total of 546 (2011) and 447 (2012) features, 29% (2011) and 24% (2012) have a duration between 0.9 and 1 hour, the remaining portion being scattered through all other durations with percentages below 2% (2011) and 3% (2012). The features occurrence along the day shows a Gaussian repartition centered around 8:30am (2011) and 9:30am (2012) with no duration correlation (R=0.09 and R=-0.1). Unfortunately, a background noise still remains after the features separation resulting in unexpected high durations. It can be explained by some isolated points distant over time then clustered together. As a consequence, only the highest duration occurrences that are related to a high confidence level can be

interpreted (here one hour). It is still important to keep in mind that some real high duration features are certainly hidden in this noise.

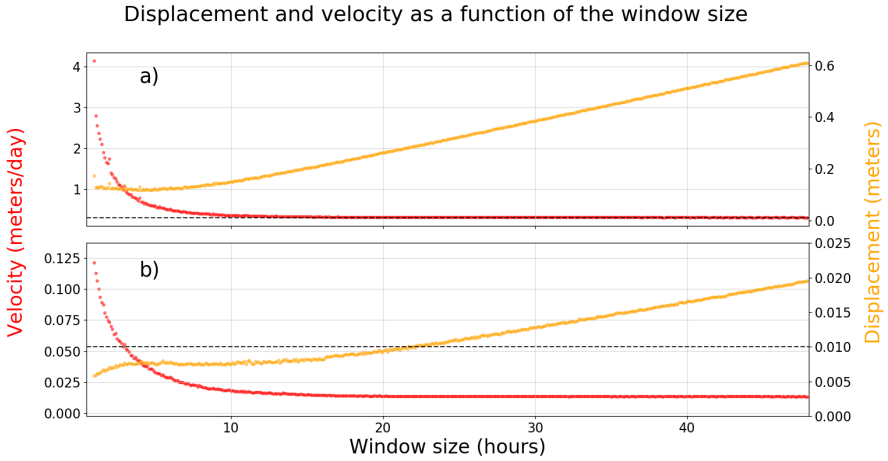

Figure 6: Displacements and velocities as a function of the window size for **a)** Holtedahlfonna ice field station (2011) and **b)** Etonbreen glacier station (2014). The minimum recordable displacement is represented by grey dashed lines.

Following these preliminary studies, the tracking of the SNR along the temporal resolution increase revealed significant non-linear decrease for all the signals (see Figure 7a) and both years. This trend can be explained by the the outliers and bad quality data influence raise but also by the appearance of real velocity variations imperceptible so far. The RF method keeps the higher SNR along the resolution increase followed by the SDF, the KMF and of the low-processed velocity. The RF method value at a twelve hours resolution in 2011, breaking the overall trend, has been assimilated to an aberrant elbow determination while filtering. The analysis in 2012 resulted in the same amplitude order. By applying the elbow method once more, a change in the 2011 data behaviour has been determined at an eight hours resolution for all the methods. This change already occurred at a twelve hours resolution in 2012 which is in line with its highly supposed lower data quality.

The percentage of missing values, for its part, follows the same order of importance where the RF method shows the higher values up to 2.7 times the SDF method except for the highest resolutions (three and one hour) where the KMF method becomes higher by 1.3 times in average (see Figure 7b). Obviously, the percentage of missing values for the low-processed velocity is equal to zero as it does not delete any data. An elbow has been determined at a twelve hours resolution for the KMF method and at an eight hours resolution for the SDF method. However, it is harder to determine a meaningful change in the data behaviour for the RF method even if an elbow has been determined at a three hours resolution. Concerning 2012, a change at eight hours has been determined for all methods.

Thus, strong anti-correlations are visible between the SNR and the percentage of missing values for all methods with R values of -0.99, -0.93 and -0.79 (2011), -0.98, -0.92 and -0.92 (2012) for respectively the KMF, SDF and RF method. The relation between these two variables could give an indication of the post-processing performance as it shows how the signal responds to the filtering.

Methods cross-comparisons revealed a Spearman correlation coefficients general decrease along the resolution increase of 2011 HDF data that shows growing divergences between the results (see Figure 8). The higher coefficients have been found between KMF and RF method which could be explained by the use of the ratio variable in both methods even if their methodologies are very different. These two methods compared to the SDF method result in lower coefficients except at a three hours timestep for the RF/SDF coefficient which remains unexplained.

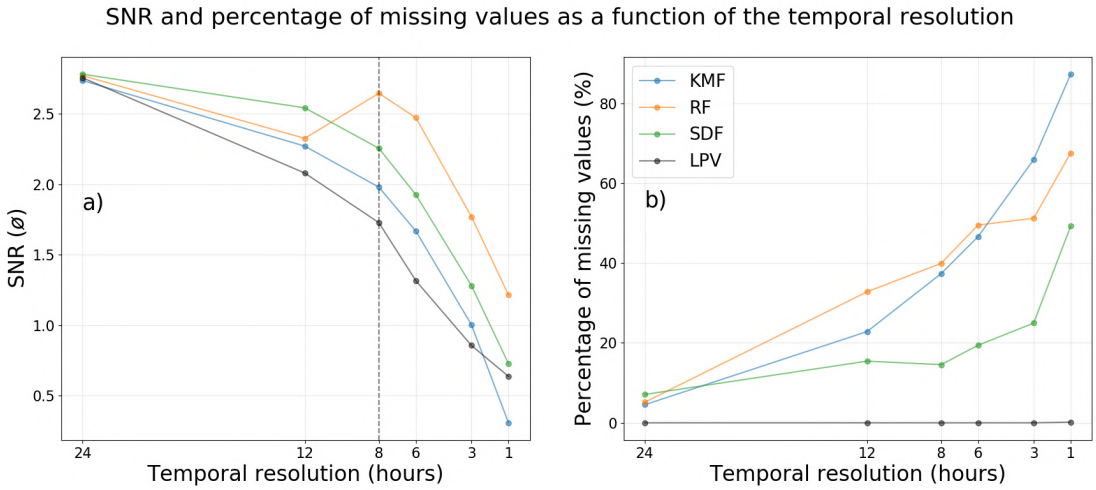

Figure 7: **a)** SNR and **b)** percentage of missing values for each method and the low-processed velocity (LPV) along the temporal resolution increase, applied to Holtedahlfonna ice field station in 2011. The change in data behaviour at an eight-hour resolution is represented by a dashed grey line.

Besides, the correlation coefficient order is reversed at a hourly resolution after a significant decrease of all the coefficients. Elbow points have been determined at three, three and eight hours resolution for respectively RF/SDF, RF/KMF and KMF/SDF. It is also visible that linear trends of all the coefficients break at a resolution of eight hours. However, stronger variations are observed at higher resolutions which explains the elbow points of RF/SDF and RF/KMF. For 2012, the only elbow determined concerned the coefficient excluding the KMF method (RF/SDF) with a change at a twelve hours resolution.

Depending on the method and the controlling variable, changes in data behaviour have been detected at different temporal resolutions. On the basis of the work here presented and in a conservative way, the highest possible temporal resolution has been fixed to the lowest resolution where significant changes has been noticed, that is to say an eight hours resolution in 2011 and a twelve hours resolution in 2012.

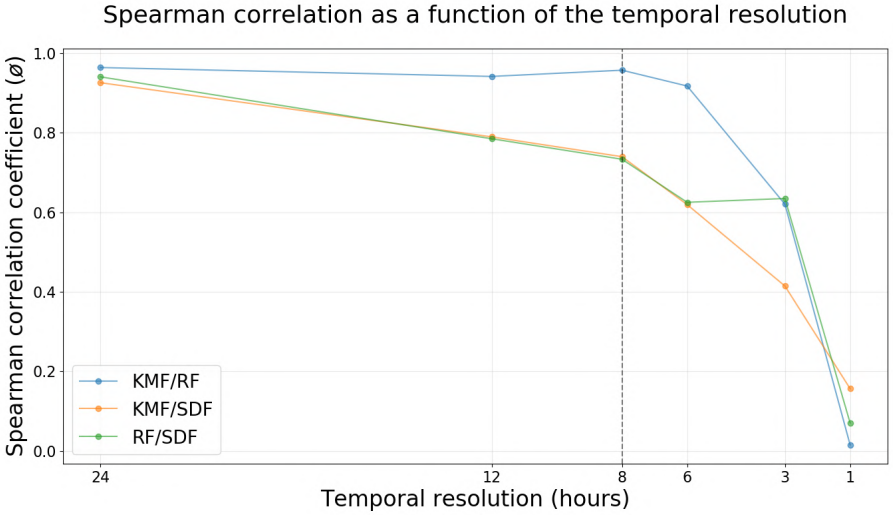

Figure 8: Spearman correlation coefficients between each method along the temporal resolution increase, applied to Holtedahlfonna ice field station in 2011. The change in data behaviour at an eight-hour resolution is represented by a dashed gray line.

5 Discussion

5.1 Contribution of melt-enhanced sliding to overall glacier displacement

Each velocity time series used in the following analysis corresponds to the mean daily velocity between the results of the three developed methods for HDF data, the only one for ETB data. Thus, for the velocity of each station, a background velocity have been fixed as the mean velocity during a pre-summer period of each record (month of May). Then, the integrative of the two curves i.e. real velocity and constant background velocity have been computed. The subtraction of the first to the second resulted in the contribution of the summer period, then normalized by the overall integrative to obtain a percentage. It is important to point out that the observed velocity has been interpolated to calculate the integrative on a closed area.

For Holtedahlfonna ice field, a contribution of 23.6 % (2011) and 22.8 % (2012) have been determined (see Figure 9a). Concerning Etonbreen glacier, despite its very slow displacement along the recording period that can suggests a relative slow melt season response, velocities 11.4 (2014) and 12.5 (2015) times superior to the background velocity have been determined (see Figure 9b). The corresponding high contributions are respectively 45.8 % and 56.7 %. By assuming that the background velocity hereby determined is close to the annual one and that no major acceleration events occurred outside the summer period, these contributions can be expanded to annual contributions.

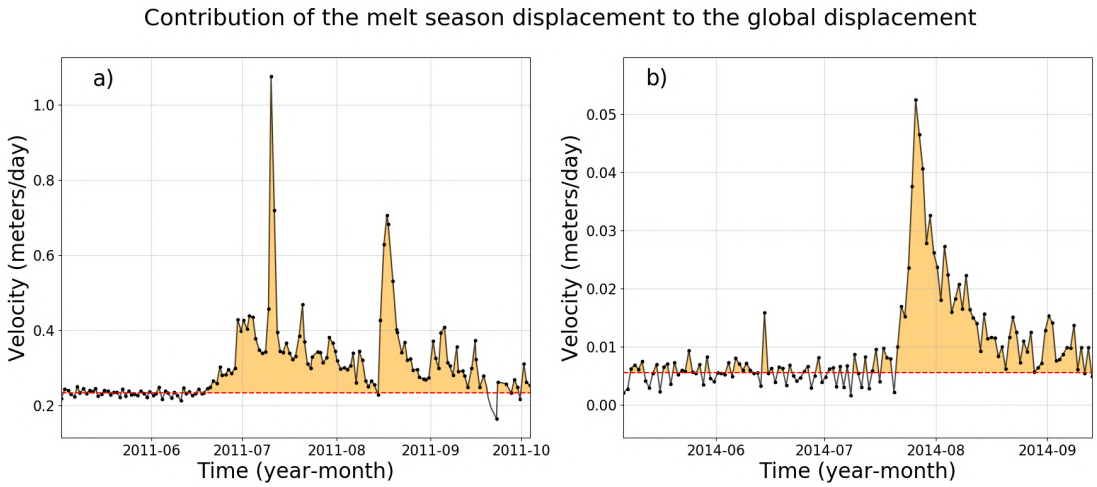

Figure 9: Mean velocity from developed methods for **a)** Holtedahlfonna ice field station in 2011 and **b)** Etonbreen glacier station in 2014. The contribution of the melt season to the overall displacement is represented by orange areas.

5.2 Glaciological interpretation

Several of the possible hypothesis are here formulated to interpret the velocity time series in relation to a potential hydrometeorological forcing. This analysis has only been led for Holtedahlfonna ice field which is the station where the data described below was available.

The outputs of DEBAM (Distributed Energy Balance Model), a coupled surface energy balance and snow pack model developed by Hock and Holmgren (2005) and Reijmer and Hock (2008) have been used. The model is forced with re-analysis climate data: ERA-40 (Fiorino et al., 2005) and ERA-Interim (Dee et al., 2011) from the European Centre for Medium-Range Weather Forecasts downscalled to 1km horizontal resolution for surface air temperature, relative humidity, winds and downwellinq shortwave and longwave radiation (Østby et al., 2017)). In this study, air temperature and precipitations from the re-analysis as well as snow/firn cover, surface melt and runoff have been investigated. Runoff occurs when water meets impermeable ice at the base of the snow/firn layer (subsurface layer),

following a bucket method wherein water spills from one grid to the next when the layer is saturated.
In 2011, an increase in air temperature in early June led to the first consecutive Positive Degree Days (PDD) and thus progressively launched the surface melt. A delay of seven days between the beginning of the surface melt and the runoff onset is visible. This delay in runoff could be due to the time it took for the snow/firn layer, unsaturated in winter, to be water saturated from surface melt and precipitations (Jansson et al., 2003). After the snowpack saturation, the runoff increased in the second part of June/early July until nearly stabilised for approximately two weeks. This two-week period also shows relatively stable velocity (see label 1 in Figure 10) when a pseudo-stable state is probably reached between surface melt/precipitations inputs and the capacity of the subglacial hydrological drainage system. Another explanation for this increase in surface velocity could be linked to a variation in the dynamics downstream (e.g. front acceleration) that propagated upstream towards the ice field.
A heavy rainfall of 17.1mm certainly triggered a speed-up event on July 10^{th} and interrupted the two-week stable velocity. While the glacial hydrological drainage system was in balance or developing upstream towards an efficient system, the surface melt and precipitations inputs redirected to the glacier bed exceeded the capacity of subglacial channels (Schoof, 2010). It certainly resulted in an increase of subglacial water pressure and thus decreased friction at the glacier base allowing the glacier to slide, generating the fastest acceleration recorded on the period (see label 2). The uplift of the glacier, most likely due to an increase in water pressure at the base as described above, could also support this hypothesis even if the vertical signal is less precise than the horizontal components.
A smaller acceleration was recorded 10 days after the heavy rainfall (see label 3) while runoff increased more than threefold over the period. A faster water transfer from the surface to the base through the firn could explain this acceleration. As firn melted, this layer progressively lost its buffer effect that delayed and reduced the transport of this water into the glacier (Reijmer and Hock, 2008). Indeed, it is visible through the new correlation between the surface melt and runoff signals once it totally melted.
The second biggest acceleration event (see label 4) in mid-August was preceded by a cold day (-2.2°C) and an important snowfall (12.6 mm w.eq.). These meteorological conditions added to a period of eight days without precipitations, a runoff decrease and a slight velocity decrease probably led to the shrinking of the subglacial hydrological system (channels) by ice deformation and reduced basal water pressure. Thus, the rapid surface melt increase during the following days and to some extent the melt of the thin snow cover had probably overloaded the low-capacity subglacial hydrological system as presented earlier for the event 2.
Finally, several but unexpectedly small accelerations occurred in September during the highest precipitation event recorded (19.8mm) as well as other rainfall events and relatively high temperature. It is hard to assess whether the GPS surface displacement reflects the real glacier displacement as the confidence on the velocity is poor at the end of the summer. Those accelerations may be real but the SNR is too low to identify the relation between glacier flow and forcing and therefore those events are not described here.
In 2012, a negative average temperature between May and August (-0.6°C versus 0.3°C in 2011) coupled to a 11% mean precipitations increase in regards to 2011 resulted in a more than twofold thicker snow cover that persisted along the summer thanks to low surface melt rates (58 % of 2011 average). The first acceleration in early July (see label 5) could have been interpreted in a similar way as the event labelled 1 in 2011. Indeed, consecutive light rainfalls resulting however in a significant cumulative water volume have been coupled to a melting period that started approximately one month before the event. However, as stated below, the snow cover remained thick along the summer resulting in an important potential water storage. Thus, for this first event, it is very unlikely that the precipitations and surface melt products reached the bed at this point as visible through the absence of runoff. Nevertheless, an uplift of the glacier have been recorded suggesting the presence of water at the base. Thus, the hypothesis of a drainage of supraglacial lakes upstream could be formulated. This process has been observed at this location by Bahr (2015) at the same time of the year (between the 10^{th} and the 12^{th} of July 2015) generating a similar acceleration response. Where a comparable drainage could be the cause of event 6 and 7, it is important

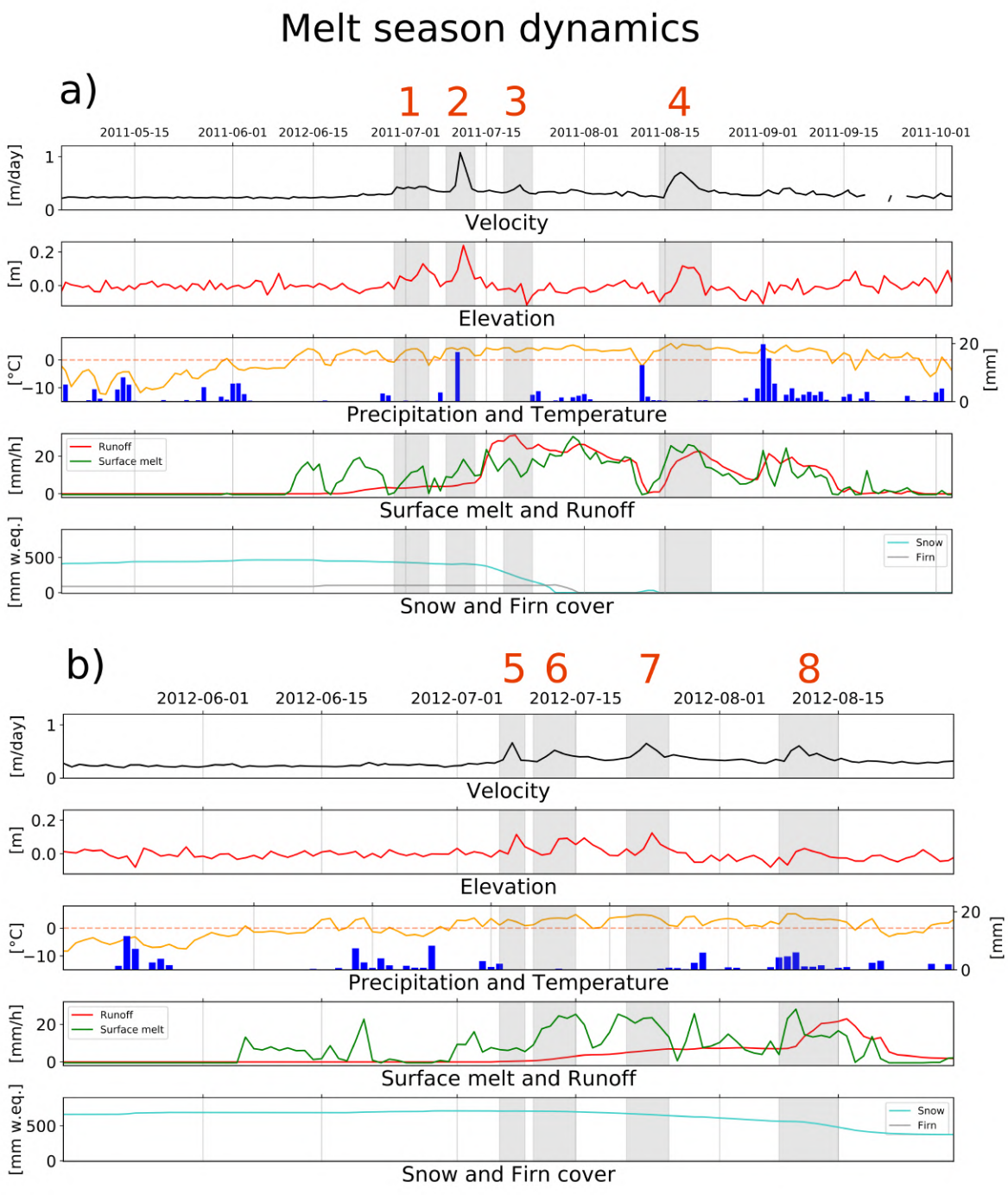

Figure 10: Mean velocity from developed methods for Holtedahlfonna ice field station in **a)** 2011 and **b)** 2012 compared to outputs of the surface mass balance model described in Section 5.2. The elevation has been detrended and thus represents the residuals of the Z component linear regression. Events discussed in Section 5.2 are labelled in orange and highlighted by grey areas.

to notice the surface melt increase and runoff onset, the products having potentially reached the bed through very low-developed crevasses and moulins. Finally, after a relatively steady velocity period in late July/early August, repeated rainfalls coupled to temperature increase may have triggered event 8, breaking the ongoing stability state as described for event 2.

5.3 Improvements and perspectives

In order to further increase the level of confidence on the post-processed data, the methods still have to be improved. For example, the algorithm used to find the Elbow point needs to be further explored, especially the sensitivity parameter (S) which makes the determination more or less conservative. This can help to determine different levels of elbows at various scales, better describe data behaviour and thus cope with situations like the Spearman coefficients evolution characterised in Section 4.2. It also needs to be strengthened to better cope with more complicated situations with, for example, multiple possible elbows by alternating concave and convex curves shapes (step-like). Besides, the only threshold that remains in the developed methods which is on the z-score of the SDF and RF methods (fixed to 1σ) needs to be more meaningful and strengthened or ideally deleted. A way to do it could be to compute the combinations of standard deviation/ratio thresholds and z-score by optimizing the processing duration which would be much longer than at the current level of processing.
In the same goal, more methods including different concepts can be compared to have a broader view of the possible results and potentially expand changes in the data behaviour. It would also be interesting to apply the developed methods to other data set to investigate their generalisation potential. In parallel, a protocol can be developed to accurately evaluate the post-processing performances, the SNR and percentage of missing values investigation being the beginning of one possible approach. Finally, even before the post-processing, more strategies could be led and compared in a similar way as in this study to find one of the optimal processing methods and perhaps reach higher resolutions with confidence. A better linkage between the processing and the post-processing steps would also be needed to strengthen the analysis and e.g. fix a more applied precision than the one used in Section 5.1 or post-process ETB data at a higher level.

6 Conclusion

Through this experimental study, different post-processing methods have been developed and compared to existing ones to evaluate the potential of GNSS data recorded at Holtedahlfonna ice field and Etonbreen glacier, in the Svalbard archipelago. High correlation coefficients from 0.79 to 0.96 were determined between the daily velocities obtained by the different developed methods at Holtedahlfonna ice field even if some unexpected short-term deviations were observed. Due to a lack of controlling variables, only one method with a low level of post-processing have been developed for Etonbreen glacier data. Comparisons with two applied methods highlighted strong variations up to 16.7 and 59.5 times the mean velocity from developed methods (for respectively Holtedahlfonna ice field and Etonbreen glacier stations), illustrating the high sensitivity of the data to the level of post-processing. The investigation of the temporal resolution increase brought out a first change in the behaviour of the Holtedahlfonna ice field data at a resolution of 8 hours (2011) and 12 hours (2012) as a result of a significant influence of short-term variations. This analysis could not have been led with Etonbreen glacier data due to a slow representative displacement that constrained the temporal resolution to 22 hours.
Finally, a glaciological analysis combining the mean daily velocity of Holtedahlfonna ice field from developed methods and outputs of a mass-balance model already provided evidences of a relation to a hydrometeorological forcing. Further work leading to an increase of the confidence on high temporal resolution velocities would certainly constitute a big step towards a better understanding of the short-term glacier dynamics.

References

Bahr, K.: High resolution glacier dynamics from GNSS measurements on Holtedahlfonna, NW Svalbard, Master's thesis, 2015.

Bartholomew, I., Nienow, P., Mair, D., Hubbard, A., King, M. A., and Sole, A.: Seasonal evolution of subglacial drainage and acceleration in a Greenland outlet glacier, Nature Geoscience, 3, 408, 2010.

Bholowalia, P. and Kumar, A.: EBK-means: A clustering technique based on elbow method and k-means in WSN, International Journal of Computer Applications, 105, 2014.

Björnsson, H., Gjessing, Y., Hamran, S.-E., Hagen, J. O., LiestøL, O., Pálsson, F., and Erlingsson, B.: The thermal regime of sub-polar glaciers mapped by multi-frequency radio-echo sounding, Journal of Glaciology, 42, 23–32, 1996.

Błaszczyk, M., Jania, J. A., and Hagen, J. O.: Tidewater glaciers of Svalbard: Recent changes and estimates of calving fluxes, Polish Polar Research, 30, 85–142, 2009.

Christianson, K., Kohler, J., Alley, R. B., Nuth, C., and Van Pelt, W. J.: Dynamic perennial firn aquifer on an Arctic glacier, Geophysical Research Letters, 42, 1418–1426, 2015.

Church, J. A., White, N. J., Konikow, L. F., Domingues, C. M., Cogley, J. G., Rignot, E., Gregory, J. M., van den Broeke, M. R., Monaghan, A. J., and Velicogna, I.: Revisiting the Earth's sea-level and energy budgets from 1961 to 2008, Geophysical Research Letters, 38, 2011.

Cuffey, K. M. and Paterson, W. S. B.: The physics of glaciers, Academic Press, 2010.

Das, S. B., Joughin, I., Behn, M. D., Howat, I. M., King, M. A., Lizarralde, D., and Bhatia, M. P.: Fracture propagation to the base of the Greenland Ice Sheet during supraglacial lake drainage, Science, 320, 778–781, 2008.

Dee, D. P., Uppala, S., Simmons, A., Berrisford, P., Poli, P., Kobayashi, S., Andrae, U., Balmaseda, M., Balsamo, G., Bauer, d. P., et al.: The ERA-Interim reanalysis: Configuration and performance of the data assimilation system, Quarterly Journal of the royal meteorological society, 137, 553–597, 2011.

Dowdeswell, J., Benham, T., Strozzi, T., and Hagen, J.: Iceberg calving flux and mass balance of the Austfonna ice cap on Nordaustlandet, Svalbard, Journal of Geophysical Research: Earth Surface, 113, 2008.

Dunse, T., Schuler, T., Hagen, J., and Reijmer, C.: Seasonal speed-up of two outlet glaciers of Austfonna, Svalbard, inferred from continuous GPS measurements, The Cryosphere, 6, 453–466, 2012.

Dunse, T., Schellenberger, T., Hagen, J., Kääb, A., Schuler, T. V., and Reijmer, C.: Glacier-surge mechanisms promoted by a hydro-thermodynamic feedback to summer melt, The Cryosphere, 9, 197–215, 2015.

Fiorino, M., Gibson, J., Haseler, J., Hernandez, A., Kelly, G., Li, X., Onogi, K., Beljaars, A., Van, L., Berg, D., et al.: The ERA-40 re-analysis, 2005.

Flowers, G. E., Jarosch, A. H., Belliveau, P. T., and Fuhrman, L. A.: Short-term velocity variations and sliding sensitivity of a slowly surging glacier, Annals of Glaciology, 57, 71–83, 2016.

Hagen, J. O., Kohler, J., Melvold, K., and Winther, J.-G.: Glaciers in Svalbard: mass balance, runoff and freshwater flux, Polar Research, 22, 145–159, 2003.

Harper, J. T., Humphrey, N. F., Pfeffer, W. T., and Lazar, B.: Two modes of accelerated glacier sliding related to water, Geophysical research letters, 34, 2007.

Helbing, J.: Glacier dynamics of Unteraargletscher: verifying theoretical concepts through flow modeling, Ph.D. thesis, ETH Zurich, 2005.

Hinze, H. and Seeber, G.: Ice-motion determination by means of satellite positioning systems, Annals of glaciology, 11, 36–41, 1988.

Hisdal, V.: Svalbard: nature and history, 1998.

Hock, R. and Holmgren, B.: A distributed surface energy-balance model for complex topography and its application to Storglaciären, Sweden, Journal of Glaciology, 51, 25–36, 2005.

Hofmann-Wellenhof, B., Lichtenegger, H., and Wasle, E.: GNSS–global navigation satellite systems: GPS, GLONASS, Galileo, and more, Springer Science & Business Media, 2007.

Hooke, R. L., Calla, P., Holmlund, P., Nilsson, M., and Stroeven, A.: A 3 year record of seasonal variations in surface velocity, Storglaciären, Sweden, Journal of Glaciology, 35, 235–247, 1989.

Jansson, P., Hock, R., and Schneider, T.: The concept of glacier storage: a review, Journal of Hydrology, 282, 116–129, 2003.

Käsmacher, O. and Schneider, C.: An objective circulation pattern classification for the region of Svalbard, Geografiska Annaler: Series A, Physical Geography, 93, 259–271, 2011.

King, M.: Rigorous GPS data-processing strategies for glaciological applications, Journal of Glaciology, 50, 601–607, 2004.

Lefauconnier, B. and Hagen, J. O.: Surging and calving glaciers in eastern Svalbard, Norsk Polarinstitutt, 1991.

Lefauconnier, B., Massonnet, D., Anker, G., et al.: Determination of ice flow velocity in Svalbard from ERS-1 interferometric observations, 2001.

MacQueen, J. et al.: Some methods for classification and analysis of multivariate observations, in: Proceedings of the fifth Berkeley symposium on mathematical statistics and probability, vol. 1, pp. 281–297, Oakland, CA, USA, 1967.

Moholdt, G. and Kääb, A.: A new DEM of the Austfonna ice cap by combining differential SAR interferometry with ICESat laser altimetry, Polar Research, 31, 18 460, 2012.

Moholdt, G., Hagen, J., Eiken, T., and Schule, T.: Geometric changes and mass balance of the Austfonna ice cap, Svalbard, The Cryosphere, 4, 21–34, 2010.

NPI: Terrengmodell Svalbard (S0 Terrengmodell), 2014.

Nuth, C., Schuler, T. V., Kohler, J., Altena, B., and Hagen, J. O.: Estimating the long-term calving flux of Kronebreen, Svalbard, from geodetic elevation changes and mass-balance modeling, Journal of Glaciology, 58, 119–133, 2012.

Nuth, C., Kohler, J., König, M., Deschwanden, A. v., Hagen, J. O. M., Kääb, A., Moholdt, G., and Pettersson, R.: Decadal changes from a multi-temporal glacier inventory of Svalbard, The Cryosphere, 7, 1603–1621, 2013.

Østby, T. I., Schuler, T., Hagen, J. O. M., Hock, R., Kohler, J., and Reijmer, C.: Diagnosing the decline in climatic mass balance of glaciers in Svalbard over 1957-2014, The Cryosphere, 11, 191–215, 2017.

Pfeffer, W. T., Harper, J. T., and O'Neel, S.: Kinematic constraints on glacier contributions to 21st-century sea-level rise, Science, 321, 1340–1343, 2008.

Reijmer, C. H. and Hock, R.: Internal accumulation on Storglaciären, Sweden, in a multi-layer snow model coupled to a distributed energy-and mass-balance model, Journal of Glaciology, 54, 61–72, 2008.

Rogers, J. C., Yang, L., and Li, L.: The role of Fram Strait winter cyclones on sea ice flux and on Spitsbergen air temperatures, Geophysical Research Letters, 32, 2005.

Ruppel, M., Isaksson, E., Ström, J., Beaudon, E., Svensson, J., Pedersen, C., and Korhola, A.: Increase in elemental carbon values between 1970 and 2004 observed in a 300-year ice core from Holtedahlfonna (Svalbard), Atmospheric Chemistry and Physics, 14, 11 447–11 460, 2014.

Satopaa, V., Albrecht, J., Irwin, D., and Raghavan, B.: Finding a" kneedle" in a haystack: Detecting knee points in system behavior, in: 2011 31st international conference on distributed computing systems workshops, pp. 166–171, IEEE, 2011.

Schellenberger, T., Dunse, T., Kääb, A., Kohler, J., and Reijmer, C.: Surface speed and frontal ablation of Kronebreen and Kongsbreen, NW-Svalbard, from SAR offset tracking, The Cryosphere Discussions, 8, 6193–6233, 2014.

Schoof, C.: Ice-sheet acceleration driven by melt supply variability, Nature, 468, 803, 2010.

Schuler, T. V., Dunse, T., Østby, T. I., and Hagen, J. O.: Meteorological conditions on an Arctic ice cap—8 years of automatic weather station data from Austfonna, Svalbard, International Journal of Climatology, 34, 2047–2058, 2014.

Shepherd, A., Hubbard, A., Nienow, P., King, M., McMillan, M., and Joughin, I.: Greenland ice sheet motion coupled with daily melting in late summer, Geophysical Research Letters, 36, 2009.

Stocker, T. F., Qin, D., Plattner, G.-K., Tignor, M., Allen, S. K., Boschung, J., Nauels, A., Xia, Y., Bex, V., Midgley, P. M., et al.: Climate change 2013: The physical science basis, 2013.

Sugiyama, S., Sakakibara, D., Tsutaki, S., Maruyama, M., and Sawagaki, T.: Glacier dynamics near the calving front of Bowdoin Glacier, northwestern Greenland, Journal of glaciology, 61, 223–232, 2015.

Takasu, T.: RTKLIB ver. 2.4. 2 manual, RTKLIB: an open source program package for GNSS positioning, Tokyo University of Marine Science and Technology, Tokyo, 2013.

Vaughan, D. G., Comiso, J. C., Allison, I., Carrasco, J., Kaser, G., Kwok, R., Mote, P., Murray, T., Paul, F., Ren, J., et al.: Observations: cryosphere, Climate change, 2103, 317–382, 2013.

Wagstaff, K., Cardie, C., Rogers, S., Schrödl, S., et al.: Constrained k-means clustering with background knowledge, in: Icml, vol. 1, pp. 577–584, 2001.

Zwally, H. J., Abdalati, W., Herring, T., Larson, K., Saba, J., and Steffen, K.: Surface melt-induced acceleration of Greenland ice-sheet flow, Science, 297, 218–222, 2002.

7 Appendices

Characteristics of Holtedahlfonna ice field GNSS stations

Stations	Sample int. [sec]	Receiver	Antenna	Sat. signal	Location
NYA1	1	Trimble NetR8	ASH701073.1	GPS+GLO	Ny-Ålesund
NYAL	1	Trimble NetRS	AOAD/MB	GPS	Ny-Ålesund
HAGN	5	Trimble NetR8	AOAD/MT	GPS+GLO	Nunatak at Kongsvegen
HDF1	5	Trimble NetR8	TRM55971.00	GPS+GLO	Glacier
HDF2*	5	Trimble NetR8	TRM55971.00	GPS+GLO	Glacier
HDF3	5	Trimble NetR8	TRM55971.00	GPS+GLO	Glacier

Table 1: * HDF2 was installed at the end of April 2015. GLO=GLONASS. Modified after Bahr (2015)

Description of HDF data variables

Variables	Units	Description
Positioning components (X, Y, Z)	meters	East, North and Elevation components projected in UTM zone 33
Standard deviations (sde,sdu,sdn)	meters	The estimated standard deviations of the solution assuming a priori error model and error parameters by the positioning options. The sdn, sde or sdu means N (north), E (east) or U (up) component of the standard deviations
Ratio factor (ratio)	ø	The ratio factor of ratio-test for standard integer ambiguity validation strategy. The value means the ratio of the squared sum of the residuals with the second best integer vector to with the best integer vector
Number of valid satellites (ns)	ø	The number of valid satellites for solution estimation
Quality flag (Q)	ø	The flag which indicates the solution quality 1 : Fixed, solution by carrier-based relative positioning and the integer ambiguity is properly resolved. 2 : Float, solution by carrier-based relative positioning but the integer ambiguity is not resolved. 3 : Reserved 4 : DGPS, solution by code-based DGPS solutions or single point positioning with SBAS corrections 5 : Single, solution by single point positioning

Table 2: Modified after Takasu (2013)